

Deformation of Marchenko-Pastur distribution for the correlated time series

Masato Hisakado*

* *Nomura Holdings, Inc., Otemachi 2-2-2,
Chiyoda-ku, Tokyo 100-8130, Japan*

Takuya Kaneko†

†*International Christian University
Osawa 3-10-2, Mitaka,
Tokyo 181-8585, Japan*

(Dated: May 23, 2023)

Abstract

We study the eigenvalue of the Wishart matrix which is created from the time series with the temporal correlation. When there is no correlation, the eigenvalue distribution of the Wishart matrix is known as the Marchenko-Pastur distribution (MPD) in the double scaling limit. When there is the temporal correlation, the eigenvalue distribution converges to the deformed MPD which has longer tail and higher peak than the MPD. We discuss the moments of the distribution and the convergence to the deformed MPD. We show the second moment increases as the temporal correlation increases. When the temporal correlation is the power decay, we can confirm the phase transition. When $\gamma > 1/2$ which is the power index, the second moment of the distribution is finite and the largest eigenvalue is finite. On the other hand, when $\gamma \leq 1/2$, the second moment is infinite and the maximum eigenvalue is infinite.

I. INTRODUCTION

Random matrix is one of the hot topics in several fields of physics and mathematics [1]. It has the several applied fields, nuclear physics, machine learning, finance, and MIMO (multiple-input multiple-output for the wireless communication) [2–7]. For MIMO the transmission characteristic is ruled by the eigenvalues of the Wishart matrix. In fact the channel capacity is calculated by the distribution of its eigenvalues.

In this article we study the time series of the financial data. We create the Wishart matrix using these data [8, 9]. When there is no correlation in the time series of the data, the distribution of the eigenvalues of the Wishart matrix converges to the Marchenko-Pastur distribution (MPD) [10] because of the Brownian motion. In MPD case there is the assumption that the independent random variables. We discuss the convergence of the distribution of the eigenvalues of the Wishart matrix when there is the temporal correlation. Here we discuss the exponential and power decay cases. In fact in the studies in MIMO, the correlations of the random matrix are important, because we can improve the channel capacity in correlated fading environments using the large eigenvalues [11–14]. The correlation represents the distance of the array antennas. In [14] for the exponential decay case, it was conjectured that the distance between the largest and the smallest eigenvalues of the Wishart matrix increases as the correlation increases using the numerical simulations. We show this conjecture in this article.

In the time series of the financial data, the temporal correlations are important. We can observe the temporal correlations in several time series. The exponential decay corresponds to short memory and the power decay corresponds to intermediate and long memories [15]. The power decays are sometimes observed in the financial time series as the fractional Brownian motion (fBm) which includes both long and short memories [16–19] In this article we use the fBm as the power decay case for the numerical simulations.

In [20], we calculated eigenvalue distribution of the Wishart matrix and compared the moments with the MPD. Note that in the application of the random matrix to the finance, the time series of the portfolio is usually used. In this case the Wishart matrix is the correlation matrix of the portfolio. The the eigenvalue distribution of the Whishart matrix does not fit the MPD well because of the true correlation in the markets. In [5] and [6] how to separate the true correlation and noise using the random matrix theory was introduced.

Here we use the time series of one product. So, the eigenvalue distribution of the Wishart matrix fit the MPD. In this case the Wishart matrix is the correlation matrix of different time series. We show some examples in Table I and its properties are in Table VII. We can confirm the moments for time series, SOY beans, VIX, and NKY225 fit well to the MPD. On the other hand, USD/CAD, EUR/CHF, and USD/CNH do not fit well. One of the reason of the fitness for MPD is the temporal correlations. In fact times series of USD/CAD, EUR/CHF, and USD/CNH have higher temporal correlations for shortest time lag and they are 0.2 or more in the absolute value as Table II. We suppose that the process with the temporal correlations is not adopted to the MPD. Then what is the distribution instead of the MPD for these time series with temporal correlations? This problem is discussed in [7] using the methods of the free probability theory.

TABLE I. Moments for the financial time series and the MPD. μ_i is the i -th moment of the MPD. [20]

No.	Data	μ_2	μ_3	μ_4	μ_5	μ_6
	MPD	1.333 (0.000)	2.111 (0.000)	3.704 (0.000)	6.938 (0.000)	13.597 (0.000)
1	USD/CAD	1.419 (0.008)	2.448 (0.028)	4.716 (0.082)	9.732 (0.218)	21.038 (0.568)
2	EUR/CHF	1.430 (0.003)	2.494 (0.016)	4.856 (0.055)	10.113 (0.164)	22.032 (0.456)
3	EUR/GBP	1.402 (0.003)	2.385 (0.015)	4.533 (0.055)	9.237 (0.180)	19.738 (0.562)
4	SOY	1.333 (0.003)	2.111 (0.013)	3.703 (0.041)	6.933 (0.122)	13.569 (0.344)
5	VIX	1.336 (0.007)	2.117 (0.027)	3.713 (0.085)	6.960 (0.254)	13.669 (0.736)
6	NKY 225	1.324 (0.049)	2.081 (0.020)	3.637 (0.064)	6.819 (0.186)	13.433 (0.512)

TABLE II. Temporal correlation of the shortest time lag of the financial time sires

No.	1	2	3	4	5	6
Data	USD/CAD	EUR/CHF	EUR/GBP	SOY	VIX	NKY 225
Corr	-0.35	-0.33	-0.32	-0.03	-0.03	-0.08

In this article we study the effects of temporal correlations of the random variables. The temporal correlation is the exponential decay and power decays. When there are temporal

correlations, the eigenvalues converge to the deformed MPD. We show the mean of the deformed MPD does not depend on the correlation and the second moment increases as the temporal correlation increases. Hence, as the correlation increases, the distribution has the fatter tail and the higher peak. When the power decay case, we can observe the phase transition. The phases are the finite second moment and the infinite second moment phases. When $\gamma > 1/2$ which is the power index of the temporal correlation, the second moment of the distribution and the largest eigenvalue are finite. On the other hand, when $\gamma \leq 1/2$, the second moment and the largest eigenvalue are infinite. In fact there are several phase transitions which depend on the temporal correlation [21, 22]. But in these cases the transition point is $\gamma = 1$.

The remainder of this paper is organized as follows. In Section II, we introduce the time series and the creation of the Wishart matrix. In Section III, we discuss the distribution of the deformed MPD. In Section IV, numerical simulations are performed to confirm the deformed MPD. Finally, the conclusions are presented in Section V.

II. TEMPORAL CORRELATION OF TIME SERIES AND RANDOM MATRIX

In this section we introduce the Wishart matrix of the time series with the correlation. We consider the time series of a stochastic process, A_t , is the variables at the time t . Here we set the normalization,

$$E(A_t) = 0,$$

and

$$V(A_t) = 1.$$

To introduce the temporal correlation, let $\{A_t, 1 \leq t \leq T\}$ be the time series of the stochastic variables of the correlated normal distribution with the following $T \times T$ correlation matrix,

$$D_{T-1} = \begin{pmatrix} 1 & d_1 & \cdots & d_{T-1} \\ d_1 & 1 & \ddots & \vdots \\ \vdots & \ddots & 1 & d_1 \\ d_{T-1} & \cdots & d_1 & 1 \end{pmatrix}. \quad (1)$$

Here the temporal correlation function, d_t , is defined as the correlation between A_s and A_{s+t} such that

$$d_t = \text{Cov}(A_s, A_{t+s}), \quad (2)$$

in any s . Note that we use the normalization of A_t . Here we fold the time series A_t , N times, where $T = N \times L$,

$$A = (\mathbf{A}_1, \mathbf{A}_{1+L}, \dots, \mathbf{A}_{1+(N-1)L}), \quad (3)$$

where $\mathbf{A}_\mu = (A_\mu, \dots, A_{\mu+L-1})^T$, $\mu = 1, 1+L, \dots, 1+(N-1)L$, is the size N vector and \mathbf{X}^T is the transpose of the vector \mathbf{X} . \mathbf{A}_μ is the time series form μ to $\mu+L-1$. A is the $L \times N$ matrix. In the application of the random matrix to the finance, \mathbf{A}_μ usually corresponds to the different products time series, but here we use one product [5, 6].

In the matrix form we can rewrite the $L \times N$ matrix form

$$A = \begin{pmatrix} A_1 & A_{L+1} & \cdots & A_{(N-1)L+1} \\ A_2 & A_{L+2} & \ddots & \vdots \\ \vdots & \ddots & \ddots & A_{NL-1} \\ A_L & \cdots & A_{(N-1)L} & A_{NL} \end{pmatrix}. \quad (4)$$

We consider the relation between the non correlated random time series and correlated ones. Here we consider the $L \times N$ matrix A_0 for non correlated time series. The elements of A_0 are i.i.d.. Here we introduce the $L \times L$ matrix Π . The relation between the matrix A and A_0 is

$$A = \sqrt{\Pi} A_0, \quad (5)$$

where

$$\Pi = \sqrt{\Pi} \sqrt{\Pi}^T = D_{L-1}. \quad (6)$$

$\sqrt{\Pi}$ is the lower triangle matrix which is created by Cholesky decomposition [23].

Next we consider the Wishart matrix of A . The Wishart matrix is the correlation matrix $C_{i,j}$ which is the symmetric matrix and the diagonal elements are 1,

$$C_{ij} = \frac{1}{L} \sum_{k=1}^L A_{iL+k} A_{jL+k}, \quad (7)$$

where $1 \leq i, j \leq N$. Note that $C_{i,j} = C_{j,i}$, when $i \neq j$ and $C_{i,i} = 1$ because of the normalization. In the matrix form,

$$C = \frac{1}{L} A^T A = \frac{1}{L} (\sqrt{\Pi} A_0)^T \sqrt{\Pi} A_0, \quad (8)$$

where A^T is the transposed matrix of A and C is $N \times N$ matrix.

When there is no correlation case, $A = A_0$, the distribution of the eigenvalues of C converges to the Marchenko-Pastur distribution (MPS) [10] in the double scaling limit, $N, L \rightarrow \infty$ with $L/N = Q$. When there is the correlation, the distribution of the eigenvalues of C converges the distribution which is different from the MPD, the deformed MPD.

III. CONVERGENCE TO DEFORMED MARCHENKO-PASTUR DISTRIBUTION

In this section we calculate the moments of the deformed MPD. Here we consider the case $d_i \rightarrow 0$, when $i \gg 1$. It means that the temporal correlation decays as time goes by. We calculate the k -th moment of eigenvalue distribution of the Wishart matrix, C ,

$$\mu_k = \frac{1}{L^k N} \left\langle \sum_{j=1}^N (x_j)^k \right\rangle = \frac{1}{N} \left\langle \text{Tr}(C^k) \right\rangle, \quad (9)$$

where x_j is the eigenvalues of C . The moment of the MPD is in Appendix A.

i. First moment

$$\mu_1 = \frac{1}{LN} \sum_{\nu=1}^L \sum_{m=1}^N \left\langle (A_{\nu m})^2 \right\rangle = 1, \quad (10)$$

in the limit of $N, L \rightarrow \infty$ with $L/N = Q$. Note that it does not depend on the kind of the correlation decay. The mean of the distribution which does not depend on the temporal correlation is 1.

ii. Second moment

$$\begin{aligned} \mu_2 &= \frac{1}{L^2 N} \sum_{\nu_1=1}^L \sum_{\nu_2=1}^L \sum_{m_1=1}^N \sum_{m_2=1}^N \left\langle A_{m_1 \nu_1}^T A_{\nu_1 m_2} A_{m_2 \nu_2}^T A_{\nu_2 m_1} \right\rangle \\ &= \frac{1}{L^2 N} \sum_{\nu_1=1}^L \sum_{\nu_2=1}^L \sum_{m_1=1}^N \sum_{m_2=1}^N \left\langle A_{\nu_1 m_1} A_{\nu_1 m_2} A_{\nu_2 m_2} A_{\nu_2 m_1} \right\rangle = 1 + \frac{1}{Q} + \frac{2}{Q} \sum_{i=1}^2 d_i^2, \quad (11) \end{aligned}$$

in the limit of $N, L \rightarrow \infty$ with $L/N = Q$. Here we assume $d_L \sim 0$ in this limit, because

$$\left\langle A_j, A_{j+L} \right\rangle = 0,$$

in the limit $L \rightarrow \infty$. The first and second terms of Eq.(11) are for the MPD. The third term is for the temporal correlation. It is the sum of the cases, $m_1 \neq m_2$ and $\nu_1 \neq \nu_2$. It is

$$\begin{aligned} & \frac{1}{L^2 N} \sum_{\nu_1 \neq \nu_2} \sum_{m_1 \neq m_2} \langle A_{\nu_1 m_1} A_{\nu_1 m_2} A_{\nu_2 m_2} A_{\nu_2 m_1} \rangle = \frac{N(N-1)}{L^2 N} \sum_{|\nu_1 - \nu_2|} \langle A_{\nu_1 m_1} A_{\nu_2 m_1} \rangle^2 \\ & = \frac{2N(N-1)L}{L^2 N} \sum_i d_i^2 = \frac{2}{Q} \sum_{i=1} d_i^2. \end{aligned} \quad (12)$$

The second moment of Eq.(11) increases as the temporal correlation increases. Then the deformed MPD has longer tail than the MPD. When the second moment is finite, there is the finite largest eigenvalue. On the other hand, the second moment is infinite, there is the largest eigenvalue is infinite. We discuss this phase transition in the subsection for the power decay case.

A. Exponential Decay case

We consider the case, exponential decay, $d_i = r^i, 0 \leq r \leq 1$ and calculate the moments. Here we set

$$A_{t+1} = rA_t + \sqrt{1-r^2}\xi_t, \quad (13)$$

where ξ_t is i.i.d. and we can obtain the exponential decay. $\sqrt{\Pi}$ is

$$\sqrt{\Pi} = \begin{pmatrix} 1 & 0 & \cdots & 0 \\ r & \sqrt{1-r^2} & 0 & \vdots \\ r^2 & r\sqrt{1-r^2} & \sqrt{1-r^2} & 0 \\ \cdots & \cdots & \cdots & \cdots \\ r^{L-1} & r^{L-2}\sqrt{1-r^2} & \cdots & \sqrt{1-r^2} \end{pmatrix}, \quad (14)$$

and

$$D_{L-1} = \sqrt{\Pi}\sqrt{\Pi}^T = \begin{pmatrix} 1 & r & \cdots & r^{L-1} \\ r & 1 & \ddots & \vdots \\ \vdots & \ddots & 1 & r \\ r^{L-1} & \cdots & r & 1 \end{pmatrix}. \quad (15)$$

i. Second moment

The second moment is

$$\mu_2 = \frac{1}{L^2 N} \sum_{\nu_1=1}^L \sum_{\nu_2=1}^L \sum_{m_1=1}^N \sum_{m_2=1}^N \langle A_{m_1 \nu_1}^T A_{\nu_1 m_2} A_{m_2 \nu_2}^T A_{\nu_2 m_1} \rangle$$

$$= 1 + \frac{1}{Q} + \frac{2}{Q} \frac{r^2}{1-r^2}, \quad (16)$$

in the limit of $N, L \rightarrow \infty$ with $L/N = Q$. The first and second terms are for the MPD. The third term is for the deformation for the correlation.

ii. Third moment

The third moment is

$$\begin{aligned} \mu_3 &= \frac{1}{L^3 N} \sum_{\nu_1=1}^L \sum_{\nu_2=1}^L \sum_{\nu_3=1}^L \sum_{m_1=1}^N \sum_{m_2=1}^N \sum_{m_3=1}^N \langle (A_{m_1 \nu_1}^T A_{\mu_1 n_2} A_{m_2 \nu_2}^T A_{\nu_2 m_3} A_{m_3 \nu_3}^T A_{\nu_3 m_1}) \rangle \\ &= 1 + \frac{3}{Q} + \frac{1}{Q^2} + \frac{6}{Q^2} \frac{r^4}{(1-r^2)^2} + \frac{6}{Q^2} \frac{r^2}{1-r^2} + \frac{6}{Q} \frac{r^2}{1-r^2}, \end{aligned} \quad (17)$$

in the limit of $N, L \rightarrow \infty$ with $L/N = Q$. The first, second and third terms are for the MPD. The rest terms are for the deformation for the correlation. The fourth term is for the case, $\nu_i \neq \nu_j$ and $m_k \neq m_l$, where i, j, k, l are 1, 2, 3, respectively. The fifth term is for the case $m_i = m_j \neq m_k$. It is one pair of m_i which have same values. The sixth term is for the case $\nu_i = \nu_j \neq \nu_k$. It is one pair of ν_i which have same values.

iii. Fourth moment

The fourth moment is

$$\begin{aligned} \mu_4 &= \frac{1}{L^4 N} \sum_{\nu_1, \nu_2, \nu_3, \nu_4=1}^L \sum_{m_1, m_2, m_3, m_4=1}^N \langle (A_{m_1 \nu_1}^T A_{\nu_1 m_2} A_{m_2 \nu_2}^T A_{\nu_2 m_3} A_{m_3 \nu_3}^T A_{\nu_3 m_4} A_{m_4 \nu_4}^T A_{\nu_4 m_1}) \rangle \\ &= 1 + \frac{6}{Q} + \frac{6}{Q^2} + \frac{1}{Q^3} \\ &\quad + \frac{24}{Q^3} \frac{r^6}{(1-r^2)^3} + \frac{24}{Q^3} \frac{r^4}{(1-r^2)^2} + \frac{24}{Q^3} \frac{r^4}{(1-r^2)^2} + \frac{24}{Q^3} \frac{r^2}{(1-r^2)} \\ &\quad + \frac{24}{Q^2} \frac{r^4}{(1-r^2)^2} + \frac{12}{Q^2} \frac{r^2}{(1-r^2)} + \frac{24}{Q} \frac{r^2}{(1-r^2)}, \end{aligned} \quad (18)$$

in the limit of $N, L \rightarrow \infty$ with $L/N = Q$. The first four terms are for the MPD. The rest terms are for the deformation for the correlation. The fifth term is for any ν_i and m_j which do not have same values, respectively. The sixth and the seventh terms are for one pair which have same values in m_i . The eighth term is for two pairs which have same values in m_i . The ninth term is for one pair which have same values in ν_i . The tenth term is for one

pair which have same values in ν_i and one pair which have same values in m_i . The eleventh term is for two pairs which have same values in ν_i .

B. Power decay case

In this section we consider the case power decay, $d_i = 1/(i+1)^\gamma$ where γ is the power index. The second moment is

$$\begin{aligned} \mu_2 &= \frac{1}{L^2 N} \sum_{\mu_1=1}^L \sum_{\mu_2=1}^L \sum_{m_1=1}^N \sum_{m_2=1}^N \langle (A_{m_1 \mu_1}^T A_{\mu_1 m_2} A_{m_2 \mu_2}^T A_{\mu_2 m_1}) \rangle \\ &= 1 + \frac{1}{Q} + \frac{2}{Q} \sum_{i=1}^N \frac{1}{(i+1)^\gamma} \\ &\sim 1 + \frac{1}{Q} + \frac{2}{(2\gamma-1)Q}, \end{aligned} \tag{19}$$

in the limit of $N, L \rightarrow \infty$ with $L/N = Q$. When $\gamma > 1/2$, μ_2 is finite. On the other hands, $\gamma \leq 1/2$, the second moment becomes infinite. It is the phase transition and the transition point is $\gamma_c = 1/2$.

If $x_1 < \infty$ which is the largest eigenvalue and $\sum_i x_i/N \rightarrow 1$ in the limit $N \rightarrow \infty$, then $\sum_i x_i^2/N < \infty$. It means finite μ_2 . Conversely if $x_1 \rightarrow \infty$ and $\sum_i x_i/N \rightarrow 1$ in the limit $N \rightarrow \infty$, $\sum_i x_i^2/N \rightarrow \infty$. It means infinite μ_2 . Hence, we can conclude finite μ_2 corresponds to finite x_1 and infinite μ_2 corresponds to infinite x_1 . So it is also the phase transition between the finite x_1 and the infinite x_1 .

VI. NUMERICAL SIMULATIONS

In this section we confirm the conclusions of the section III using the numerical simulations.

A. Exponential Decay

i. Deformed MPD

At first we confirm the deformed MPD. We have calculated 1000 times each r and created the histogram of the eigenvalues. The conclusion are shown in Fig.1. We can confirm the distributions have a fat tail and a high peak for large r and the mean of the distribution

is constant. On the other hand for small r , the distributions are almost same shape as the MPD.

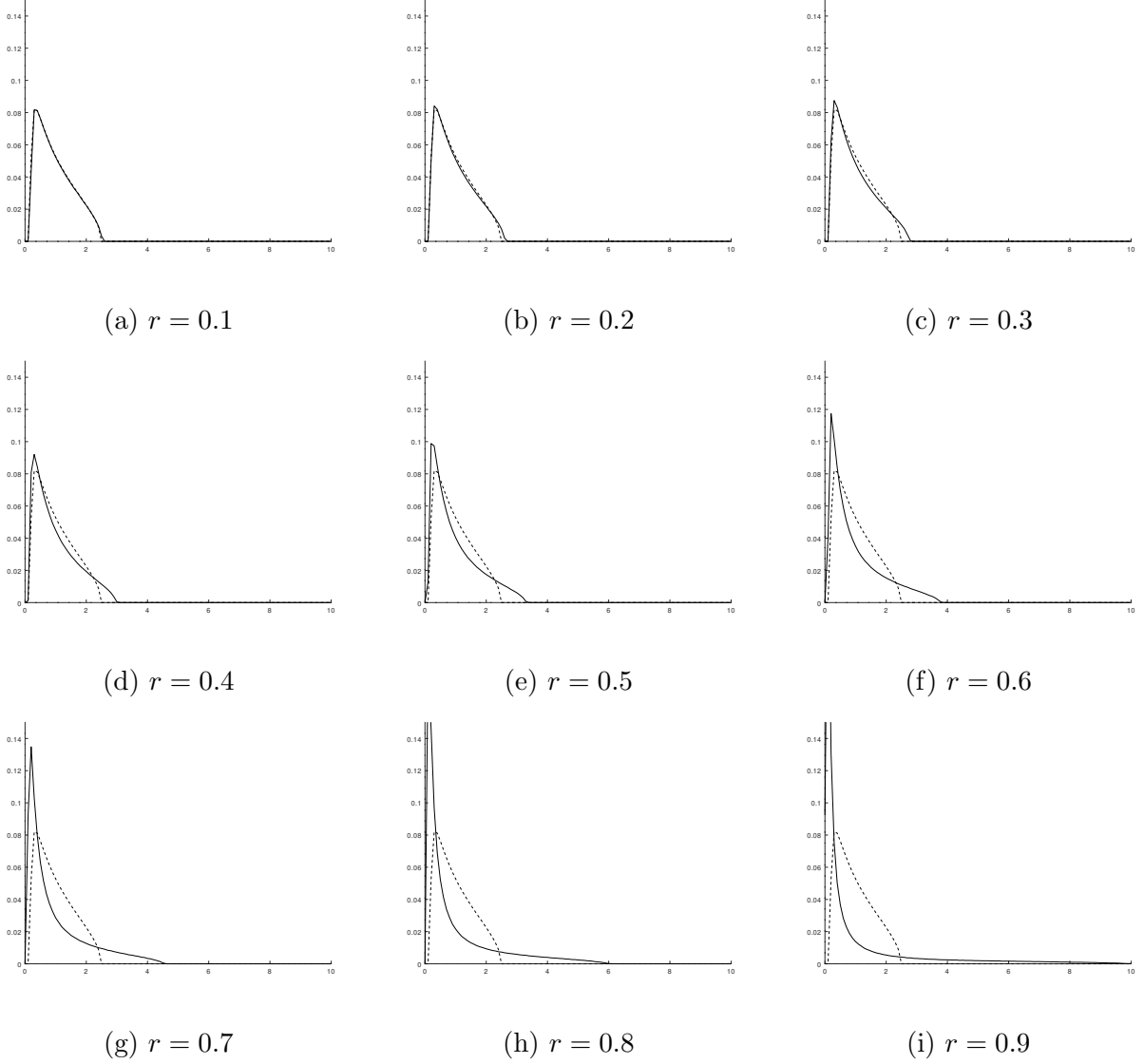


FIG. 1. Plots of the histogram of deformed MPD for $Q = 3$, (a) $r = 0.1$, (b) $r = 0.2$, (c) $r = 0.3$, (d) $r = 0.4$, (e) $r = 0.5$, (f) $r = 0.6$, (g) $r = 0.7$, (h) $r = 0.8$, (i) $r = 0.9$. The horizontal axis is r and the vertical axis is the frequency. The real line is the distribution with the correlation and the dotted line is the MPD. We can confirm the fat tail of the distribution for large r and the mean is constant.

ii. *The convergence of the moments*

Next we confirm the convergence of the distributions for the exponential decay case. In Fig.2 we show the convergence of the moments, μ_2 and μ_3 . The horizontal axis is r and the vertical axis is the second and third moments. As the matrix size increases the moments converges to the theoretical ones. In the Appendix.C. we show the conclusions of the numerical simulations in detail.

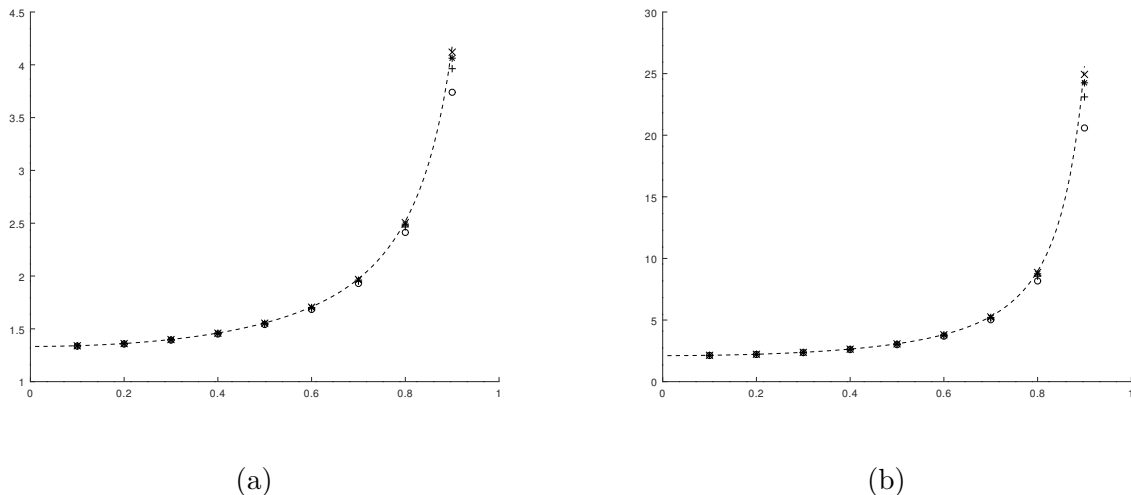


FIG. 2. The left figure is the concentration of μ_2 and the right figure is the concentration of μ_3 . The horizontal axis is r and the vertical axis is the second and third moments. Line styles: "o", "+", "*", "x", and the dotted lines indicate $N = 64, 128, 256, 512$ and theoretical moments, respectively. As the matrix size increases the moments converge to the theoretical ones. Curves are average of 1,000 times replication and the moments are the averages.

B. Fractional Brownian motion

Next we confirm the fractional Brownian motion (fBm) case which has the power decay temporal correlations and the fBm is observed in the financial time series. The relation of the indexes is

$$2 - 2H = \gamma, \tag{20}$$

where H is the Hurst index for the fBm and γ is the power index. Hence, the transition point is $H_c = 3/4$ which corresponds to $\gamma_c = 1/2$. We explain the fBm in Appendix B.

i. Deformed MPD

At first we confirm the distributions of the deformed MPD for the fBm case. We have calculated 100 times each H and created the histogram of the eigenvalues. The conclusion are shown in Fig.3. We can confirm the difference form the MPD in smaller H and larger H . On the other hand for around $H = 0.5$, the distributions are almost same shape as the MPD, because $H = 1/2$ is the Brownian motion.. Above $H_c = 3/4$, there is the phase transition and we can observe the large eigenvalues. In fact we can observe the peak at 10 in $H = 0.8, 0.9$ Fig.3 (h) and (i) which corresponds to the large eigenvalues above 10.

ii. Convergence of the moments

Next we confirm the convergence of the distributions for fBm case. In Fig.4 we show μ_2 in $Q = 3, 6$ below $H_c = 3/4$ which is the transition point. Above $H_c = 3/4$, the second moment diverges. The horizontal axis is H and the vertical axis is the second moment. As the matrix size increases the moments converges to the theoretical ones. In the Appendix.C. we show the conclusions of the numerical simulations in detail.

iii. Largest eigenvalue

Next we confirm the largest eigenvalue. In Fig. 5 we show the largest eigenvalues which are average of 100 calculations when $Q = 3$ and $Q = 6$. We can confirm the sudden increase of the largest eigenvalues around $H_c = 3/4$ which is the transition point.

VI. CONCLUDING REMARKS

We considered the time series with the correlation and its Wishart matrix. When the variables are independent the eigenvalue distribution of the Wishart matrix converges to the Marchenko-Pastur distribution (MPD). When there is the correlation, the eigenvalue distribution converges to the deformed MPD. The deformed MPD has the long tail and the high peak for large temporal correlations. We calculated the some moments of the distribution and discussed the convergence of this distribution. We have shown the mean of the distribution does not depend on the correlation and the second moment increases as the

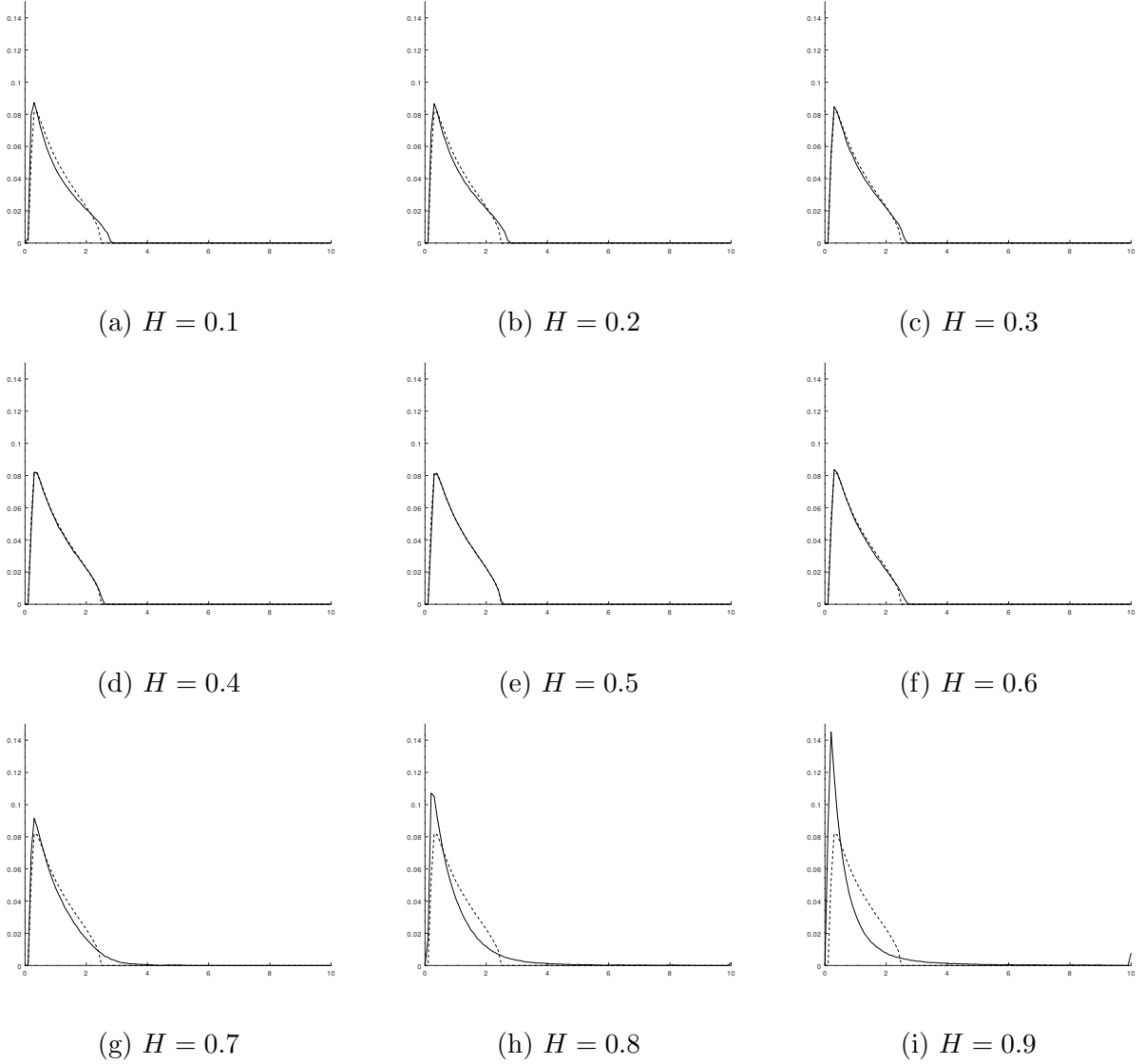


FIG. 3. Plots of the histogram of deformed MPD for $Q = 3$, in the case of fBm (a) $H = 0.1$, (b) $H = 0.2$, (c) $H = 0.3$, (d) $H = 0.4$, (e) $H = 0.5$, (f) $H = 0.6$, (g) $H = 0.7$, (h) $H = 0.8$, (i) $H = 0.9$. The horizontal axis is r and the vertical axis is the frequency. The real line is the distribution with the correlation and the dotted line is MPD. We can confirm the fat tail distribution for large H and small H .

temporal correlation increases. Especially when the temporal correlation is the power decay, we can confirm the phase transition from the finite second moment to the infinite second moment. In other words it is the phase transition between the finite largest eigenvalue to the infinite largest eigenvalue. If $\gamma > 1/2$ which is the power index, the second moment of the distribution and the maximum largest are finite. On the other hand, when $\gamma \leq 1/2$,

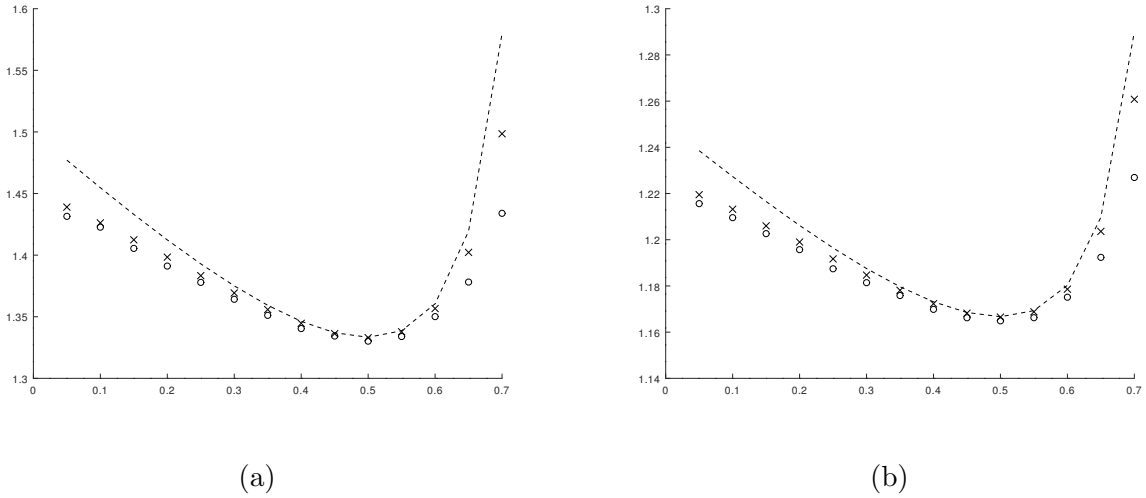


FIG. 4. The figure (a) is μ_2 in $Q = 3$ and the figure (b) is $Q = 6$ in the case of fBm. They are the comparisons between the theoretical moments and $N = 512$ numerical simulations. The horizontal axis is H and the vertical axis is the second moment. "x", "o" indicate $N = 512, 64$ and the dotted lines show the theoretical moments.

the second moment and the largest eigenvalue are infinite. The largest eigenvalues and the explicit formula of deformed MPD are the future problems.

APPENDIX A. THE MARCHENKO-PASTUR DISTRIBUTION AND ITS MOMENTS

In this Appendix A. we calculate the moments of the Marchenko-Pastur distribution (MPD). The MPD is

$$P(\lambda) = \frac{Q}{2\pi\lambda} \sqrt{(\lambda_+ - \lambda)(\lambda - \lambda_-)},$$

where

$$\lambda_{\pm} = 1 + \frac{1}{Q} \pm 2\sqrt{\frac{1}{Q}},$$

and

$$Q = \frac{L}{N},$$

in the limit $N, L \rightarrow \infty$ with constant Q .

We can obtain the moment of the MPD

$$\mu_k = E(\lambda^k) = \int_{\lambda_-}^{\lambda_+} \lambda^k P(\lambda) d\lambda$$

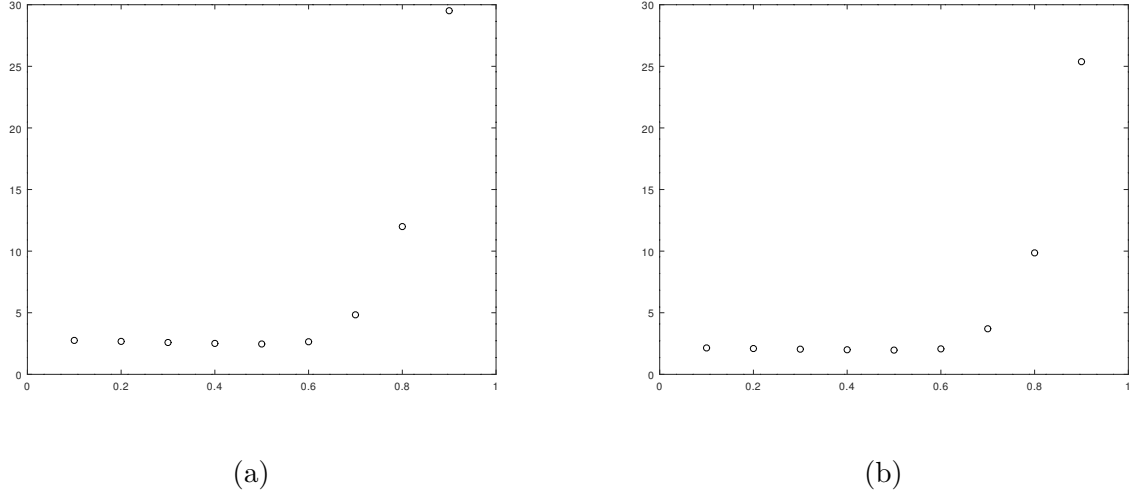


FIG. 5. The figure (a) is the maximum eigenvalue in $Q = 3$ and $Q = 6$ in the case of fBm. They are the $N = 512$ numerical simulations. The horizontal axis is H and the vertical axis is the second moment. "o" indicate $N = 512$.

$$= \frac{2}{\pi} \int_{-1}^1 [2\sqrt{\frac{1}{Q}}x + (1 + \frac{1}{Q})]^{k-1} \sqrt{1-x^2} dx, \quad (21)$$

where

$$x = \frac{\lambda - (1 + \frac{1}{Q})}{2\sqrt{\frac{1}{Q}}}.$$

Here we divided the cases when $k = 2m + 1$ and $k = 2m + 2, m = 1, 2, \dots$.

In the case $k = 2m + 1$, we expand the first term by x and the odd powers of x become 0,

$$\begin{aligned} \mu_k &= \sum_{i=0}^m \binom{2m}{2i} C_i (1 + \frac{1}{Q})^{2m-2i} \frac{1}{Q^i} \\ &= \sum_{j=1}^k \sum_{i=0}^m \binom{2m}{2i} \binom{2m-2i}{j-1-i} C_i \frac{1}{Q^{j-1}} \\ &= \sum_{j=1}^k \frac{1}{k} \binom{k}{j} \binom{k}{j-1} \frac{1}{Q^{j-1}} \end{aligned} \quad (22)$$

$$= \sum_{j=1}^k N(k, j) \frac{1}{Q^{j-1}} = \mathcal{N}_k(\frac{1}{Q}) \quad (23)$$

$N(k, j)$ is the Narayana number and $\mathcal{N}_k(x)$ is the Narayana polynomial. Then, the momentum of the MPD is the Narayana polynomial.

In the first first equal we use the relation

$$\int_{-1}^1 x^{2i} \sqrt{1-x^2} dx = \frac{\pi}{2^{2i+1}} C_i,$$

and C_i is the i the Catalan number

$$C_i = \frac{1}{i+1} \binom{2i}{i}. \quad (24)$$

In the second equal we use $j = i + l + 1$ instead of l . In the third equal we use the following identity,

$$\frac{1}{k} \binom{k}{j} \binom{k}{j-1} = \sum_{i=0}^{\lfloor (k-1)/2 \rfloor} \binom{k-1}{2i} \binom{k-2i-1}{j-1-i} C_i. \quad (25)$$

When $k = 2m + 2$ we can obtain in the same way

$$\begin{aligned} \mu_k &= \sum_{i=0}^m \binom{2m+1}{2i} C_i \left(1 + \frac{1}{Q}\right)^{2m+1-2i} \frac{1}{Q^i} \\ &= \sum_{j=1}^k N(n, j) \frac{1}{Q^{j-1}} = \mathcal{N}_k\left(\frac{1}{Q}\right). \end{aligned} \quad (26)$$

In summary we can obtain the moment μ_k for the MPD as Narayana polynomial,

$$\begin{aligned} \mu_1 &= 1 \\ \mu_2 &= 1 + \frac{1}{Q} \\ \mu_3 &= 1 + \frac{3}{Q} + \frac{1}{Q^2} \\ \mu_4 &= 1 + \frac{6}{Q} + \frac{6}{Q^2} + \frac{1}{Q^3} \\ \mu_5 &= 1 + \frac{10}{Q} + \frac{20}{Q^2} + \frac{10}{Q^3} + \frac{1}{Q^4} \\ \mu_6 &= 1 + \frac{15}{Q} + \frac{50}{Q^2} + \frac{50}{Q^3} + \frac{15}{Q^4} + \frac{1}{Q^5}. \\ &\dots \end{aligned} \quad (27)$$

APPENDIX. B FRACTIONAL BROWNIAN MOTION

$H \in (0, 1)$ is the parameter of the fractional Brownian motion (fBm). When the Gauss process $B^H = \{B_t^H\}_{t \geq 1}$ with $E(B^H) = 0$ satisfies following condition, the process is the fBm,

$$\text{Cov}(B_s^H, B_t^H) = \frac{1}{2} (|t|^{2H} + |s|^{2H} - |t-s|^{2H}), \quad (28)$$

in any t and s . H is the Hurst index. In the case $H = 1/2$, the process is the Brownian motion. In the case $H \neq 1/2$, the process has the power decay temporal correlation with $\gamma \sim 2 - 2H$ in $t \gg 1$. Here γ is the power index. Hence, when $H > 1/2$, the process has long memory and $H < 1/2$ the process has short memory.

APPENDIX C. CONVERGENCE TO THE THEORETICAL VALUES OF THE DEFORMED MPD

In this section we compare the theory and the numerical simulations. We show the cases $Q = 3$ and $Q = 6$ of exponential decay temporal correlation in Table.III and Table.IV, respectively. In Table.V and Table.VI we show the cases of the fBm in $Q = 3, 6$. At $H = 3/4$ μ_2 becomes infinite.

TABLE III. Comparison of the moments between the simulations and theory for $Q = 3$

r	0	0.1	0.2	0.3	0.4	0.5	0.6	0.7	0.8	0.9
$N = 512, \mu_2$	1.3329	1.3396	1.3605	1.3984	1.4591	1.5537	1.7053	1.9681	2.5047	4.1215
Theory μ_2	1.3333	1.3401	1.3611	1.3993	1.4603	1.5556	1.7083	1.9739	2.5185	4.1754
$N = 512, \mu_3$	2.1092	2.1362	2.221	2.3775	2.6378	3.0651	3.8058	5.2536	8.8539	24.9533
Theory μ_3	2.11111	2.13812	2.22338	2.38137	2.64324	3.07407	3.82205	5.28861	8.95885	25.59588
$N = 512, \mu_4$	3.698	3.7792	4.0378	4.5286	5.3836	6.8831	9.746	16.1855	36.184	173.524
Theory μ_4	3.70370	3.80732	4.13587	4.75033	5.78594	7.53909	10.73691	17.59557	38.10822	180.77500

APPENDIX D. PROPERTIES OF THE FINANCIAL TIME SERIES DATA

Table VII is the properties of the data in the section I.

* hisakadom@yahoo.co.jp

TABLE IV. Comparison of the moments between the simulations and theory for $Q = 6$

r	0	0.1	0.2	0.3	0.4	0.5	0.6	0.7	0.8	0.9
$N = 512, \mu_2$	1.1671	1.1698	1.1802	1.1992	1.2295	1.2771	1.3532	1.4853	1.7554	2.5731
Theory μ_2	1.16667	1.17003	1.18056	1.19963	1.23016	1.27778	1.35417	1.48693	1.75926	2.58772
$N = 512, \mu_3$	1.5294	1.5386	1.5753	1.6432	1.7536	1.9322	2.2326	2.7954	4.1076	9.418
Theory μ_3	1.52778	1.53958	1.57668	1.64479	1.75605	1.93519	2.23676	2.80254	4.12860	9.53055
$N = 512, \mu_4$	2.1756	2.1986	2.2924	2.4685	2.7634	3.2614	4.1568	6.0069	11.0852	39.8625
Theory μ_4	2.17129	2.21626	2.35784	2.61857	3.04684	3.74331	4.93717	7.25797	13.15499	43.86338

TABLE V. Comparison of the moments between the simulations and theory for fBm in $Q = 3$

H	0.1	0.2	0.3	0.4	0.5	0.6	0.7	0.8	0.9
$N = 512, \mu_2$	1.4261	1.3982	1.369	1.3448	1.3331	1.3568	1.4991	2.1279	4.7319
Theory	1.454	1.412	1.375	1.346	1.333	1.360	1.579	N.A.	N.A.

† tkaneko@icu.ac.jp

[1] M.L. Mehta, *Random matrices* (3rd edition) , Elsevier (2004).

[2] G. Akemann, J. Baik, and P.Di Francesco (Editors), *The oxford Handbook of Random Matrix Theory*, Oxford Univ.Press (2011)

TABLE VI. Comparison of the moments between the simulations and theory for fBm in $Q = 6$

H	0.1	0.2	0.3	0.4	0.5	0.6	0.7	0.8	0.9
$N = 512, \mu_2$	1.2130	1.1989	1.1846	1.1723	1.1663	1.1787	1.2603	1.7062	3.9633
Theory	1.227	1.206	1.188	1.173	1.1667	1.180	1.290	N.A.	N.A.

TABLE VII. data spec

no.	data name	data category	data period	data interval	data length
1	USD/CAD	FX (natural resource)	2021/5/19 20:22-2021/7/15 19:57	minutely	60,000
2	EUR/CHF	FX (cross pair)	2021/5/18 13:20-2021/7/15 20:00	minutely	60,000
3	EUR/GBP	FX (cross pair)	2021/5/19 1:06-2021/7/15 20:00	minutely	60,000
4	SOY beans	commodity	2021/4/19 9:01-2021/7/15 19:57	minutely	38,483
5	VIX	commodity	2021/4/15 20:11-2021/7/15 19:56	minutely	48,106
6	NKY225	stock index	1965/1/5-2021/7/15	daily	14,886

- [3] D.C. Hoyle and M. Rattray, *Phys. Rev. E* **69(2)** 026124 (2004)
- [4] T Hastie, A. Montanari, S. Rosset, and R.J. Tibshirani, *Annals of Stat* **50(2)** 949
- [5] L. Laloux, P. Cizeau, J.-P. Bouchaud, and M. Potters *Phys Rev. Lett.* **83** 1467 (1999)
- [6] M. Potters and J.-P. Bouchaud *Theory of Financial Risk and Derivative Pricing: From Statistical Physics to Risk Management* Cambridge university press (2003)
- [7] M.Potters and J.-P. Bouchaud *A first course in random matrix theory* Cambridge university press (2021)
- [8] J. Wishart, *Biomet* **20A** 32 (1928)
- [9] R.A.Fisher. *Biomet* **10(4)** (1915)
- [10] V.A. Marčenko and L.A. Pastur *Math of USSR-Sbornik* **1(4)** 457 (1967)
- [11] M. Chiani, M.Z. Win, and A.Zenella, *IEEE Trans. Inf. Theory* **49(10)** 2363 (2003)
- [12] S.H.Simon, A.L. Moustakas, and L. Marinelli, *IEEE Trans. Inf. Theory* **52(12)** 5336 (2006)
- [13] V.V. Veeravalli, Y. Liang, and A.M. Sayeed, *IEEE Trans. Inf. Theory* **51(6)** 2058 (2005)
- [14] Y.Karasawa, *IEEE Trans. Vehicul. Technol* **69(5)** 5330 (2020)
- [15] I. Florescu, M. C. Mariani, H. E. Stanley, and F. G. Viens (Eds.) *Handbook of High-Frequency Trading and Modeling in Finance* John Wiley& Sons (2016)
- [16] F. Biagini, Y. Hu, B. Øksendal, and T Zhang *Stochastic calculus for fractional Brownian motion and applications* Springer Science and Business Media (2008)
- [17] S. Rostek, R Schöbel *Econ Modeling* **30** 30 (2013)
- [18] B.B. Mandelbrot and J.W. Van Ness, *SIAM rev* **10(4)** 422 (1968)
- [19] M T Greene and B D Fielitz *J. Fin Econ* **4(3)** 339 (1977)

- [20] T. Kaneko, M Hisakado, *Random Matrix Theory (RMT) Application on Financial Data* In: Aruka, Y. (eds) *Digital Designs for Money, Markets, and Social Dilemmas. Evolutionary Economics and Social Complexity Science* **28** Springer 347 (2022)
- [21] M. Hisakado and S. Mori, *Physica A*, **544** 123480 (2020)
- [22] M Hisakado, S Mori *Physica A* **563**, 125435 (2021).
- [23] J.P. Kermoal, L. Schumacher, K.I. Pedersen and P. Mogensen *IEEE J. Selec. Areas. Commun* **20(6)** 1211 (2002)